The MIT Super Mini Cheetah: A small, low-cost quadrupedal robot for dynamic locomotion

Will Bosworth[1], Sangbae Kim[1], and Neville Hogan[1,2]

***Abstract*— We present the MIT Super Mini Cheetah, a small (sub-10kg) and low-cost (sub-10k$) quadrupedal robot for dynamic locomotion. The robot can control vertical and horizontal force and impedance at each foot and performs dynamically stable walking, jumping, pronking, turning and braking using simple force and impedance trajectories. We present design specifications for dynamic legs which were used to guide the selection of leg components (e.g., motor, gearbox, and limb geometry). We demonstrate experimental evidence of accurate force control during foot-ground impact and present video of locomotion gaits performed by the robot. To the best of our knowledge, this is the first small (sub-10kg), power autonomous quadrupedal robot to perform such a wide range of ballistic locomotion behaviors and demonstrate foot force control during impact.**

I. Introduction

As highlighted by the recent DARPA Robotics Challenge [1], exploration, clean-up and rescue over dangerous terrain are important applications for robotic legged locomotion which remain unsolved. Physical robots play a critical role in controller development for legged locomotion, particularly for running and jumping where hard-to-model impact and friction dynamics significantly affect system performance. Because of the challenge in accurately modeling ground properties, the gap between present-day simulation and real-robot performance increases as terrain becomes more uneven and unpredictable—which is the environment that legged robots should provide the most value. If they have sufficient dynamic capability, smaller and lower cost robots enable more robot testing over wider terrain types. Such empirical study is needed to bridge the gap between simulation and real robot capability.

We introduce the MIT Super Mini Cheetah (SMC), a small (sub-10kg) and low-cost (sub-10k$) quadrupedal robot. For its size and cost the robot is unique in its ability to accurately control force and impedance between each foot and the ground, as well as generate sufficient force and motion for many dynamic behaviors. For example, the robot has jumped higher than its own leg length and performed gaits such as pronking, turning, and walking. The purpose of this paper is to describe the SMC robot design, show its ability to control leg forces, and demonstrate initial dynamic behaviors achieved by the robot. These capabilities show that the SMC robot is suitable for locomotion testing in a variety of environments.

Corresponding author bosworth@mit.edu

[1]Author is with the Department of Mechanical Engineering, Massachusetts Institute of Technology, Cambridge, MA 02139.

[2]Author is with the Department of Brain and Cognitive Science, MIT.

Fig. 1: The Super Mini Cheetah (SMC) robot: a small quadrupedal robot capable of power-autonomous dynamic behaviors such as walking, jumping, bounding, turning and stopping.

A. Related work

Motivated by the high force density requirements of locomotion, many legged robots use actuators with high intrinsic inertia and friction. Model-based inverse dynamics, often incorporating force sensors at the end of the limb, is one approach to control limb force with high intrinsic inertia actuators [2][3]. While inverse dynamic models can be accurate at low speeds, they are unable to cancel inertial effects during large accelerations due to practical bandwidth limitations of the actuator and power electronics. Non-collocated force control also exacerbates the possibility of contact instability [4]. Furthermore, these methods require time-consuming system identification, which reduces the speed of iterative design of the hardware.

Series elastic elements are often used in robot legs that are powered by actuators with high intrinsic inertia [5]-[9]. Some modern quadrupeds such as Starleth [8] use the Series Elastic Actuator paradigm [10] to control foot forces. Other modern robots such as the Cheetah-Cub [6] use elastic elements to store and release energy throughout the gait cycle. In these cases, an important role of series elasticity is to shape the dynamic response of ground impact. However, selecting the best leg impedance for different behaviors remains an open research problem and modulating the impedance of a series-elastic leg often requires iterations of mechanical hardware which can be prohibitively time consuming. On-going research in variable impedance actuators is attempting to address this limitation [11].

Robot arms such as the Phantom haptic interface have used rigid links powered by current-controlled electric mo-

tors [12]. This design paradigm can result in limbs with low intrinsic inertia and friction which is necessary to perform accurate force and impedance control during mechanical impact, though achieving sufficient torque density for dynamic legged robots is challenging. The MIT Cheetah is the only well known robot that extends this design paradigm to a power-autonomous legged robot that can perform fast running and dynamic maneuvers [13]-[15], though its custom motors and components make it an expensive platform to replicate at present. Some legged robots use rigid limb links powered by hydraulic actuators. These systems have increased mechanical system complexity and are quite large—in excess of 70 kg for quadrupeds[1] [16][17].

Motivated by the success of the MIT Cheetah, we developed the SMC robot to achieve smaller size, lower cost and faster iteration time by emphasizing the use of commercial-off-the-shelf components and rapid prototyping methods. To describe our design specification and initial experimental results, this paper proceeds as follows:

- Section II presents the design requirements of a leg for accurate force and impedance control and force density required for jumping and landing.
- Section III presents an overview of the SMC robot and the controller used to achieve the open-loop behaviors (jumping, bounding, turning, walking and stopping).
- Section IV presents experimental data of the SMC robot: control of both vertical and horizontal ground force during static standing; control of vertical ground force during jumping; force and body motion during steady hopping in place. A video of a variety of locomotion behaviors is included.
- Section V presents conclusions and future work.

II. The Design Requirements of a Dynamic Leg

A leg design for dynamic locomotion must balance requirements such as control fidelity, force density, range of motion, and avoidance of failure modes that arise from foot-ground impact and the thermal losses of actuation. This section draws on experimental biology and simple dynamic models to develop a specification for the mass-specific force, impedance, and motion needed for a leg that can perform dynamic locomotion.

A. Accurate force control with forward kinematics

Robots that perform accurate force control without inverse dynamics can greatly simplify control system design and implementation. In order to use a kinematic approximation of a limb to accurately relate motor torque to limb force, the actuators must be able to generate accurate torques and the non-kinematic terms that are present in the dynamics of the limb must be minimized.

Consider the dynamics of a planar n-DoF rigid body model:

$$D(q)\ddot{q}+C(q,\dot{q})\dot{q}+G(q)+f_c(q,\dot{q},\tau)=\tau+J^T(q)F_{ext} \quad (1)$$

[1]Design specifications and performance of Boston Dynamics' robots are not widely available in academic literature. Their size is publicly available.

where $q,\dot{q} \in R^n$ are the generalized coordinates/velocities, $D(q)$ is the inertia matrix, $C(q,\dot{q})$ is the Coriolis and centrifugal term, $G(q)$ is the gravity vector, $f_c(q,\dot{q},\tau)$ is the friction, τ is the input control torques, $J(q)$ is the kinematic Jacobian matrix, and $F_{ext} \in R^2$ is the horizontal and vertical ground reaction force vector.

A low-inertia leg that acts as a perfect force source generates forces through interaction with the ground by directly relating motor torque and the leg Jacobian, as described by Eq 2.

$$-\tau \approx J^T(q)F_{ext}. \quad (2)$$

In real robots, this dynamic approximation can be accurate during relatively low accelerations and when inertia and friction are minimized. Therefore, the approach cannot control forces upon impact against the ground but may approximate desired force during the ground contact phase when acceleration is relatively small. The Jacobian relationship is only accurate if the connecting links between the torque source and the foot are rigid. If there is significant intrinsic compliance (damping or stiffness), these energy storage elements must also be considered to describe the leg dynamics. Gear transmission ratios must be minimized, as inertia and viscous friction in the motor are reflected onto the limb by the square of the gear ratio and dry fiction—i.e., modeled by Coulomb friction—is reflected by the first power of the gear ratio.

B. Limb force and motion during ground contact

The limb forces required for locomotion can be estimated using observations from experimental biology as well as simple momentum analysis. A wide variety of legged locomotors exhibit patterned vertical ground reaction force profile shapes during locomotion; the profile resembles a half sine wave, often with additional high frequency dynamics at the initiation of impact. The amplitude of the profile typically increases with forward speed, but the vertical limb force during high speed steady running has been measured between two to three body weights for a variety of animals [18][19][20].

The force profile required for a given system mass, stride time, and stance time can be estimated using the principle of momentum balance using a simplified shape of the force profile [20]. In steady state running, the integral of the vertical ground reaction force that acts on a body mass must equal the integral of the gravity force through the duration of the stride:

$$\int_0^T f_y(t)\,dt = m\,g\,T \quad (3)$$

where T is the stride time, f_y is the vertical ground reaction force acting on the body, m is the body mass, g is gravity and t is time.

If the ground reaction force profile is approximated as a half sine wave with peak amplitude A and stance time t_{stance}, as in Eq 4,

$$f_y(t) = A \sin \frac{\pi\, t}{t_{stance}} \quad for \;\; 0 < t < t_{stance} \tag{4a}$$

$$f_y(t) = 0 \quad for \quad t \geq t_{stance} \tag{4b}$$

then the peak amplitude of the force profile can be estimated by calculating the integral analytically:

$$A = \frac{m\, g\, T\, \pi}{2\, t_{stance}}. \tag{5}$$

Eq 5 describes how to estimate the peak forces that must be generated by the legs (peak amplitude A) for a given system mass, stride time and stance time. The difference between stride time T and stance time t_{stance} is the time that the body would spend in flight with no legs on the ground. The value A can be divided between multiple legs with simple arithmetic.

Intrinsic to the nature of mechanical work, locomotion requires limbs to exert both force and motion to move a torso [21]. A survey of locomotors shows that the vertical travel of a limb during locomotion is typically about 20% of the total limb length [22]. The vertical limb motion $l(t)$ during stance can be approximated as a half sine wave with an amplitude Δl_{max} and stance time t_{stance}.

$$l(t) = \Delta l_{max} \sin \frac{\pi t}{t_{stance}} \tag{6}$$

With this approximation, the peak vertical velocity of the limb, $v_{y,max}$, is estimated as,

$$v_{y,max} = \frac{\Delta l_{max} \pi}{t_{stance}}. \tag{7}$$

The rotational speed of the hip joint during stance can be estimated as the quotient of the forward running speed and the length of the leg.

C. Limb stiffness and damping before and during ground contact

Mechanical impedance control is used widely on robots involved in intermittent mechanical contact, of which legged locomotion is a flagship example. While there is no consensus that pure impedance control is the most appropriate method to approach locomotion, many studies have shown that tuned limb impedance can aid robust, stable, and energetically efficient locomotion [2,5-9,13-15]. In particular, there appears to be significant opportunity to combine direct force profile control with tuned limb impedance [15].

If a limb can adequately approximate a force source, as discussed in Sec II-A, then impedance of the limb can be commanded as a function of the position and velocity of the limb. For example, the vertical foot force that results from impedance control, $f_{y,imp}$ [N], can be commanded as a function of stiffness gain K_y [N/m] and damping gain B_y [Ns/m] as a function of deviation from a nominal leg length Δy [m], and deviation from nominal leg velocity Δv_y [m/s] [23].

$$f_{y,imp} = K_y\, \Delta y + B_y\, \Delta v_y \tag{8}$$

The maximum achievable stiffness and damping through active control depends on the bandwidth of the actuator's torque (or force) control, the precision and accuracy of the measurement of foot kinematics (Δy and Δv_y), the bandwidth of the control computer, and the intrinsic impedance of the leg structure.

While the best range of impedances for high performance locomotion remains an open research problem, the peak limb stiffness required for locomotion can be estimated from studies of experimental biology [18]. The role of limb damping is less documented; the damping ratio of limbs in large mammals has been observed to approach zero, while damping ratios of 0.2-0.3 have been measured in smaller insects [24].

We estimate that a useful lower limit of damping in a hopping machine would be one in which the forces generated during stance through the limb are negligible compared to the desired forces that should be exerted on the body to move. For brevity, we acknowledge that a sufficiently transparent limb designed to the requirements in Sec II-A will have adequately low intrinsic damping.

D. Limb motion during swing

The speed of swing-leg motion is dependent on a limb's force capability[2], inertia and intrinsic friction. The amount of time available for swing leg return actions is related to the stride frequency and duty cycle of a gait. We draw on observations of biology to estimate the typical times and motions available for this action [18][19][20].

The required torque and operating speeds for the swing leg motion can be estimated assuming a simple bang-bang controller. The magnitude of the torque required to swing the leg forward, τ_s, is given in Eq 9. This value is dependent on limb rotational inertia I_{leg}, swing time t_{swing}, and leg angle to be swept $\Delta\theta_s$.

$$\tau_s = \frac{4\, \Delta\theta_s\, I_{leg}}{{t_{swing}}^2} \tag{9}$$

From Eq 9, the peak joint speed to return the leg after stance, $\omega_{s,max}$, is shown in Eq 10.

$$\omega_{s,max} = \frac{\tau_s\, t_{swing}}{2\, I_{leg}} \tag{10}$$

E. The workspace of the leg

The functional workspace of a leg includes the range of motion of the limb and the positions over which the forces required for locomotion can be generated. A wide range of animals use hip rotations of +/- 30° from vertical during ground contact [18]. Vertical travel of the limb during ground contact has been observed to be 20% of the limb length [22].

[2]Stored elastic energy could be released during recirculation, which could be considered part of the available force/torque for the limb action.

F. Mechanical failure

The primary mechanical failure modes in a robot leg are structural failure due to high impact forces, and thermal failure of the motors due to heat dissipation. All elements in the drivetrain including gear teeth, bearings, structural connections and rigid links must be able to withstand the cyclic loads generated during ground contact. The forces required for locomotion discussed in Sec II-B provide a baseline for the load requirements of the limb structure. The design requirements introduced in Sec II-A also help to minimize the impact forces upon contact with the ground. Introduction of foot compliance mitigates impact forces but compromises the force control bandwidth of the leg.

In an electric motor, thermal failure is caused by heat that is generated while creating large torques. The heat power generated as a function of motor current and motor resistance is given in Eq 11, where P_{joule} is the Joule heating power [W], i_m is motor current, and R_m is motor resistance.

$$P_{joule} = {i_m}^2 R_m. \tag{11}$$

Using thermal characteristics provided by the manufacturer, the designer should write a safety algorithm that keeps the estimated temperature of the motor below the operating temperature. This algorithm typically requires estimating the RMS current through the motors.

To estimate the RMS motor current that would be used to achieve a jumping gait of desired stride time and stance time, we combine the ground-force estimates of Eqs 3-5, the relationship of motor torque and foot force in Eq 2, a motor's torque constant k_m and gear transmission ratio G_m, and the Jacobian of the leg. The required torque for swing leg return (Eq 9) could also be included, but we note that a leg designed with intrinsically low inertia will not require significant swing-leg torque for many behaviors.

Recalling Eqs 3-5, the amplitude of vertical force A can be calculated from the stance time t_{stance}, the body mass m and the desired stride time T. Having calculated amplitude A in Eq 5, the required vertical force profile $f_y(t)$ would follow the half-sine wave shape of Eq 4.

The motor current i_m required to generate a vertical force is a function of the motor's torque constant k_m [Nm/A], the gear transmission ratio G_m connected to the motor and the leg Jacobian[3] J_y which acts as an additional transmission from motor torques to foot force. The instantaneous vertical force f_y as a function of motor current and leg properties is:

$$f_y = k_m i_m G_m J_y(q) \tag{12}$$

The RMS current $i_{m,RMS}$ is found by equating the vertical force in Eq 12 to the required vertical force profile that follows from Eqs 4 and 5. Using the half sine wave approximation of Eq 4 and a constant, conservative estimate of the vertical Jacobian, $J_y^\dagger$, the required current profile can be solved analytically. The resulting RMS motor current over the stride interval T is shown in Eq 13. The value for A and the RMS torque may be dependent on the number of legs and the number of motors used per leg.

$$i_{m,RMS} = \left(\frac{A}{k_m\, G_m\, J_y^\dagger}\right)\sqrt{\left(\frac{t_{stance}}{2\,T}\right)} \tag{13}$$

[3]In a planar leg, the Jacobian J has horizontal and vertical components. In Eqs 12 and 13, J_y corresponds to the vertical components of the Jacobian.

III. The Super Mini Cheetah Robot

A. Leg design: motor and structure

The SMC robot leg draws on the design of the MIT Cheetah robot which uses low-gear ratio electric motors connected by rigid limb links. A solid model of a single SMC robot leg is shown in Fig 2. Two DC motors are mounted in a single housing, which is then mounted to the torso of the quadruped. The rigid links of the leg couple the outputs of the two motor shafts to the foot, creating a five-bar closed chain linkage which has been seen in robots such as ATRIAS [7]. This parallel motor layout allows both motors to share vertical and horizontal foot forces, decreasing the motor torques needed to support high vertical loads, which decreases the motor shaft radial load requirements. The links are manufactured using 3d printed ABS plastic; the rotational joints of the links are made with plain bearings and shoulder screws. Each foot contains a contact sensor made using a pressure sensor embedded in rubber [25].

The design of the leg proceeded iteratively following the process described in Fig 3, which refers to the design requirements in Sec II. First, a candidate motor and gearbox was selected which appeared to have adequate torque, inertia, friction, and load capacity. The mass of the motor determined an estimate of the total mass of a quadruped. This estimated mass was used to calculate the required force and motion capabilities of the limb, which enabled a search for adequate limb geometry. Detailed design of limb links was guided by structural loading requirements (Sec II-F). Verification of the thermal loading was performed using the approximation described in Eq 13 as well as dynamic simulation of single leg hopping and quadrupedal bounding. Table I lists the commercial-off-the-shelf components used in the SMC robot.

B. Leg design: Power electronics and computation

Implementing endpoint force and impedance control on the SMC robot leg requires accurate measurement of the motor shaft positions and a high-bandwidth control computer to calculate the configuration dependent leg Jacobian in real-time and calculate feedback motor torques. Each motor is driven by a high-bandwidth current controller and fitted with a precise motor encoder. A microcontroller is used to read sensors, perform computation, and send torque commands to each motor; the total loop time during quadrupedal locomotion is approximately 350 μs. The current controllers provide accurate current tracking at better than 1 kHz.

C. Quadrupedal robot design

The SMC robot (Fig 1) was built after first testing a single leg and a planar-constrained biped robot (with one front and rear limb). The quadruped contains four identical leg

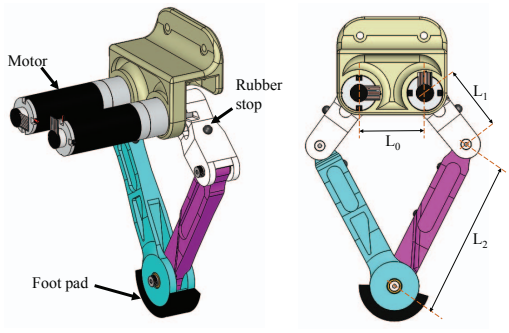

Fig. 2: A rendering of the SMC leg. Two motors are mounted on the "shoulder" which attaches to the torso (not shown). The leg structure consists of four rigid plastic links, resulting in a 5-bar linkage leg. The dimensions of the leg are: $L_0 = 60$, $L_1 = 60$, $L_2 = 145$ mm.

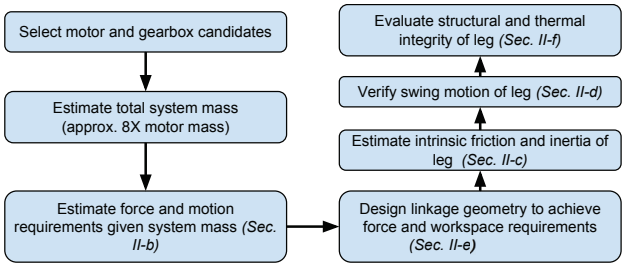

Fig. 3: A block diagram of the design process used to guide the selection and evaluation of a motor, gearbox, and limb geometry for the SMC robot leg.

TABLE I: Off-the-shelf electromechanical parts used in the robot

Component name	Manufacturer part
Motor	Faulhaber 3272, 32mm ϕ
Gearbox	Faulhaber 32-3S, 23:1
Shaft encoder	CUI AMT103
Current controller	Maxon Escon Module 50/5
Microcontroller	Cypress PSoC 5LP
Battery	Thunderpower 70C 325 mAh 3S; (8x)
Inertial measurement unit	Vectornav VN-100 Rugged

modules attached to a rigid torso frame built from aluminium extrusion, and a PCB designed to hold the eight current controllers and the microcontroller. Two 12-cell (44.4 V nominal) battery packs were assembled from smaller COTS 3-cell LiPo batteries; the drive electronics of the front and rear legs operate on independent battery packs in order to limit the voltage drop across a single battery pack.

The complete SMC robot, including batteries, weighs approximately 9 kg. The limbs are 30 cm apart in length and 18 cm apart in width. The leg length can range from 10 to 20 cm.

D. Control system design

The gaits presented in this paper are controlled using force and impedance commands to individual legs; the commands are organized by sequential state machines which are triggered by timers or ground contact sensing, as in Fig 4. Prior work has demonstrated stable locomotion with simple controllers that primarily rely on impedance (e.g., [6][14][26]). Other hardware studies have shown that active force and impedance control concepts can be combined to exploit advantages of both approaches (e.g., [15]). The experiments performed in this work are used primarily to demonstrate the dynamic capability of the new SMC robot, though the ability to extend a simple force and impedance controller to a variety of behaviors—both forward motion and turning—provides further evidence for the potential to control locomotion using both force and impedance commands.

A bound gait is characterized by synchronized ground contact of the front limbs and rear limbs respectively. The forward and turning bounding gaits use single-leg state machines which define swing and stance phases, shown in Fig 4. The front and rear limb pairs are synchronized by coupling the ground contact state of both limbs – for example, if either front limb enters the ground state the other limb must also enter the ground state.

A simple design methodology is used to select the force and impedance commands to be applied during the ground contact states:

1) Open-loop force profiles are designed to achieve desired open-loop behavior (as in Eqs 4 and 5).
2) Joint impedance, applied in parallel to the force profile, provides a spring-damper "suspension" to stabilize the open-loop behavior.

Vertical force profiles were designed using the concepts described in Sec II-B for hopping and running. Forward motion was generated by applying positive horizontal force profiles to the legs, while turning was achieved by treating the horizontal force profiles like a "tank-drive" system: if limbs on the left side push forward, and limbs on the right side push backwards, a net turning moment will be applied to the machine. Impedance was selected empirically using a simple simulation model and the SMC robot; prior research [27] and high-speed video analysis provided useful insight to select the impedance.

Some important locomotion behaviors, such as performing braking from a drop test or forward running, may be better described using only limb impedance control. A three-legged walking gait, which could be implemented if one leg failed, was quickly designed by moving sequentially through statically stable poses that were achieved using only limb impedance commands.

IV. Hardware Experiments

This section presents experimental data of the SMC robot performing force control during static standing and during hopping. We describe tests to characterize the impedance range of the limb. Additionally, experimental data of body

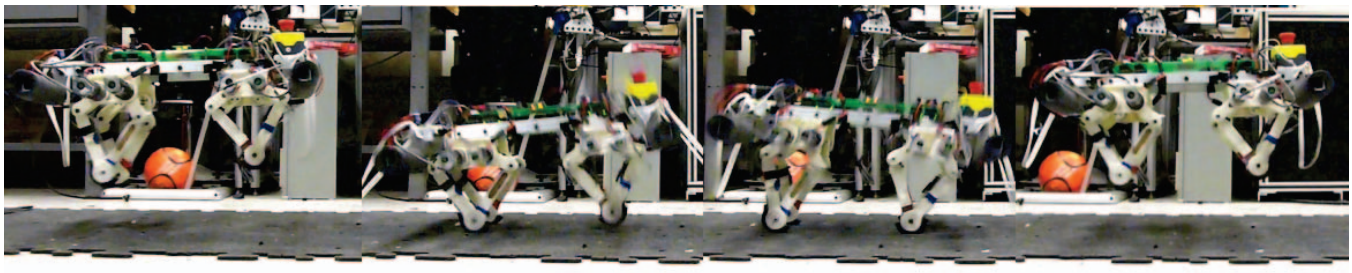

Fig. 5: Time-lapse of the SMC robot performing a pronking gait, taken at intervals of 0.167 s.

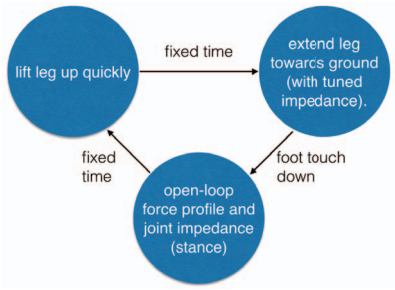

Fig. 4: Schematic of the single-leg state machine used to organize swing and stance phases for the bounding and turning behaviors described in this paper. Each state contains a single position command and set of impedance gains; the stance phase also contains an open-loop force profile for vertical and horizontal forces. The sequential progression between the states is shown by the arrows; the arrow text describes each exit condition. Individual leg state machines can be combined by coupling state transitions: in a bound, if one front foot touches the ground (initiating the stance state), the other front foot will also begin its stance state.

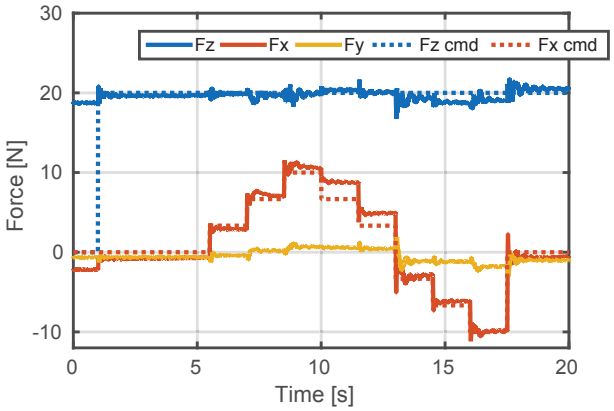

Fig. 6: The results of a static force testing experiment measuring the performance of one leg while the SMC robot was standing upright. A constant vertical force (F_z) was commanded and the horizontal force (F_x) followed a simple pattern of step commands. The dotted lines describe the commanded foot forces and the solid lines show measured force. The results show that vertical and horizontal force can be commanded independently, though there is hysteresis in the horizontal force.

rotation, leg kinematics, and motor torque are shown during a hopping gait. A **video attachment** of the the SMC robot performing a variety of gaits is included with this paper submission. A time-lapse of one such running gait is shown in Fig 5.

A. Force control during standing

Static force tests of the limb were performed to test the ability of the leg to independently command vertical and horizontal ground forces. In these tests, the robot was standing on four legs unconstrained by any additional supports, with one leg in contact with a multi-axis load cell (ATI SI-660-60). The robot could stand upright on three legs by commanding static position and impedance setpoints to these limbs. The fourth limb, which was standing over the load cell, was then free to command forces. A constant vertical force was commanded to push the foot into the ground and a simple pattern of horizontal forces was commanded. The magnitude of the horizontal force was selected so that the foot would not slip; the magnitude of the vertical force was selected to be approximately a quarter of the machine body weight (20 N) so that the robot would stand still.

Fig 6 shows vertical and horizontal ground reaction forces measured by an external load cell as well as the commanded forces. The data shows that vertical force and horizontal force can be commanded independently of each other and that the forces generally track the commanded value, though hysteresis is visible in the horizontal force output.

B. Leg impedance range

Swing-leg motion profiles were used to characterize the leg impedance. In these tests, the body was fully constrained and the limb was not touching the ground. A lumped parameter model of the leg was estimated by measuring the natural frequency and damping ratio of the step response of the motor joint for a variety of stiffness gains (Eq 8). The reflected damping and inertia of the vertical travel of the foot with respect to the body is estimated as 13.3 Ns/m and 2.3 kg respectively. The intrinsic limb impedance is configuration dependent; these impedance values represent the leg at a length of approximately 15 cm, halfway between its maximum length of 20 cm and minimum length of 10 cm. Though experiments verifying the accuracy of the limb impedance at the foot have not been performed, the leg can

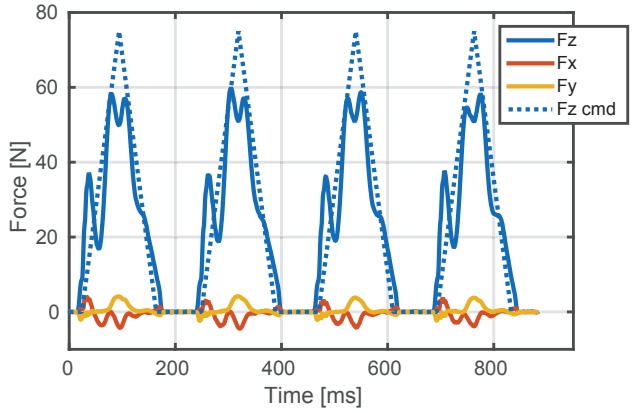

Fig. 7: The results of a vertical hopping test, showing the performance of one leg. The data shows four consecutive stance events. The dotted line shows the vertical force command; commanded horizontal force was zero. The results show that measured ground reaction force (F_z) follows the commanded force with some additional high frequency content, and the horizontal force (F_x) and out-of-plane force (F_y) remain near the desired zero magnitude.

generate stable impedance commands corresponding to 4 kN/m stiffness and 4 kNs/m damping.

C. Force control during hopping

Fig 7 shows the commanded and measured ground forces during a vertical hopping experiment. In this trial the two back legs were commanded to stand upright using constant position and impedance setpoints. The two front limbs used controllers described in Fig 4: when the foot sensor measured ground contact (which requires approximately 10N) each leg commanded a feed-forward ground force trajectory. No additional impedance command was used during the stance state. The force trajectory only contained vertical force; the horizontal force command was zero.

The data in Fig 7 shows four consecutive steps of the two-leg hopping behavior. The measured ground reaction force resembles the commanded force profile in both duration and magnitude, with some high-frequency content in the measured ground force.

D. Body motion, leg motion, and motor current during hopping

Fig 8 shows data that was acquired on-board the SMC robot while performing hopping in place on all four legs. The data shows 11 strides of data over approximately three seconds—data acquisition is limited by memory on the microcontroller. Data was acquired at 250 Hz. This gait was controlled using a controller as described in Fig 4, though the two front legs and two rear legs were coupled together—i.e., if one front leg detected ground contact, both legs would enter the stance control state. Though the front and rear legs were not synchronized in the controller, the resulting gait resembled a pronking gait.

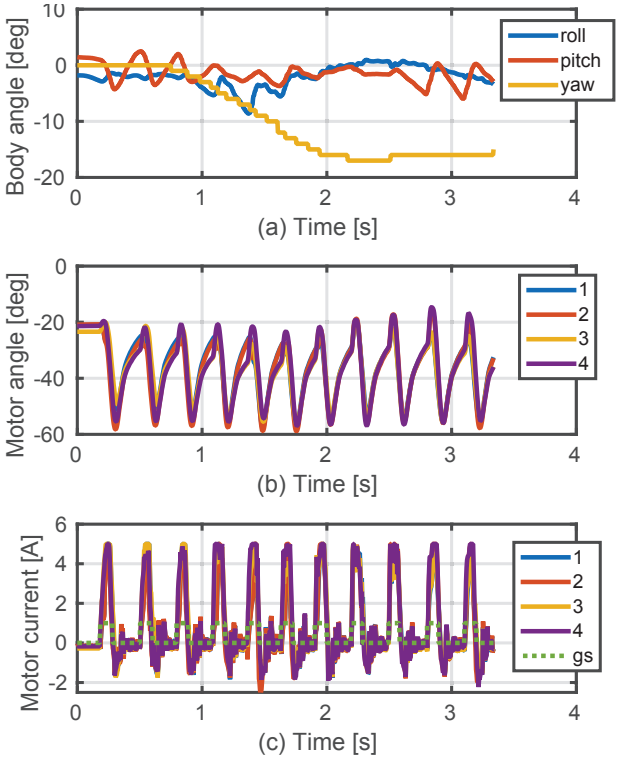

Fig. 8: Data acquired on board the SMC robot during hopping. (a) shows the angular orientation of the body and shows that yaw angle (heading) is not well regulated. (b) shows motor angles for the four motors of the front limbs (motors 1 and 2 are part of one leg; 3 and 4 another). (c) shows the commanded motor current during jumping; the dashed line shows the result of one ground contact sensor (the ground contact sensor is a boolean value and scaled to fit the other values on the graph). The data shows that the robot can hop persistently using RMS motor currents below 2 A, which is within the ratings of the motors and drive components.

Fig 8 shows body orientation (roll, pitch and yaw). The data shows that pitch and roll angle were regulated to within +/-5 degrees of horizontal. The yaw angle (heading) exhibits drift as it is not regulated in the present controller. Angle and torque of four motors (two for each of the front legs) shows approximately 40 degrees of travel of each limb and a peak current of 5 A. During this experiment, each leg was in contact with the ground for about 0.1 s for each 0.18 s of flight time.

E. Bounding, turning, braking and walking

Numerous gaits have been performed using the controller described in Sec III-D; a time lapse of one forward pronking stride is shown in Fig 5. Forward gaits were achieved using stance times of between 100 and 200 ms with stride frequencies on the order of 3 Hz. Amplitude of the vertical force profile in each leg (as in Eq 4) was between 60 to 80 Nm and satisfactory gaits were found using vertical limb

impedances from 1 to 1.5 kN/m and up to 60 Ns/m. Forward speeds of nearly 1 m/s were achieved. Though rigorous characterization of stability has not been performed, the robot exhibits dynamic stability in roll and pitch directions which can be observed in the video attachment. The heading orientation of the quadruped is not yet controlled with feedback, though intentional turning can be controlled by modifying the horizontal forces of the forward bounding gait to apply a net turning motion on the torso. Turning rates of $\frac{\pi}{3}$ rad/s were achieved.

The machine can perform repeatable braking maneuvers by switching to an impedance-only control for each limb's stance phase. Applying a limb impedance command of 1.2 kN/m and 60 Ns/m brought turning and bounding gaits to rest within a single step. Additionally, walking gaits have been developed using impedance trajectories only.

V. Conclusion & Future Work

We developed the SMC quadrupedal robot to address the opportunity that small, low-cost, dynamic robots can play in understanding locomotion: empirical robot study is of particular use for hard-to-model environments such as highly cluttered and variable terrain. The SMC robot was made with commercial-off-the-shelf electromechanical components and modern rapid prototyping methods to decrease cost and increase replicability. We demonstrated the robot leg's ability to perform force and impedance control during locomotion and showed the dynamic capability of the robot with data acquired by the robot while performing hopping as well as with video demonstration. The benefit of limbs that are capable of force and impedance control is made apparent by the variety of locomotion behaviors that were demonstrated with a very simple design methodology. The ability to generate such a variety of gaits bodes well for using the SMC robot to study gaits on numerous terrain types and environments.

Immediate continued work includes characterizing the stability of open-loop gaits such as those described in this paper, as well as further integrating state estimation to enable complete model-based feedback control. Further characterization of the force and impedance control of the leg on different ground surface types is ongoing. We intend for the SMC robot to be a platform for a broad range of legged applications; as such, we documented the mechanical requirements of the limb to provide a guide for further iteration of the leg platform for different dynamic locomotion goals or size scales.

VI. Acknowledgements

The authors thank the DARPA Maximum Mobility and Manipulation (M3) Program and the Louis G. Siegle Fellowship for supporting this work.

The authors thank Jonas Whitney, Debbie Ajilo, Michael Farid, and Michael Chuah for significant contributions to the SMC robot development.

References

[1] "What Is the DARPA Robotics Challenge (DRC)?", DARPA Robotics Challenge., n.d. Web. 10 July 2015, http://www.theroboticschallenge.org/overview.
[2] Sreenath, K., et al. "A compliant hybrid zero dynamics controller for stable, efficient and fast bipedal walking on MABEL." IJRR (2011).
[3] Grebenstein, M, et al. "The DLR hand arm system." IEEE ICRA 2011
[4] Eppinger, S, and Seering W. "Understanding bandwidth limitations in robot force control." ICRA 1987.
[5] Saranli U., Buehler M., and Koditschek D., "RHex: A simple and highly mobile hexapod robot." IJRR 20.7 (2001): 616-631.
[6] Sprwitz, Alexander, et al. "Towards dynamic trot gait locomotion: Design, control, and experiments with Cheetah-cub, a compliant quadruped robot." IJRR 32.8 (2013): 932-950.
[7] Grimes, Jesse A., and Jonathan W. Hurst. "The design of ATRIAS 1.0 a unique monoped, hopping robot." CLAWAR 2012.
[8] M. Hutter, C. Gehring, M. Bloesch, M. Hoepflinger, C. D. Remy, R. Siegwart, StarlETH: A Compliant Quadrupedal Robot for fast, efficient, and versatile Locomotion, Proc. of the International Conference on Climbing and Walking Robots (CLAWAR), 2012.
[9] Raibert, Marc, et al. "Bigdog, the rough-terrain quadruped robot." Proceedings of the 17th World Congress. Vol. 17. No. 1. 2008.
[10] Pratt, Gill, and Matthew M. Williamson. "Series elastic actuators." IEEE/RSJ IROS 1995.
[11] Vanderborght, Bram, et al. "Variable impedance actuators: A review." Robotics and Autonomous Systems 61.12 (2013): 1601-1614.
[12] Salisbury, K., and Srinivasan M. "Phantom-based haptic interaction with virtual objects." Computers Graphics and Applications, IEEE 17.5 (1997): 6-10.
[13] Seok, S, et al. "Design principles for highly efficient quadrupeds and implementation on the mit cheetah robot." IEEE ICRA 2013.
[14] Hyun, Dong Jin, et al. "High speed trot-running: Implementation of a hierarchical...", IJRR 33.11 (2014): 1417-1445.
[15] Park, H, Chuah M, and Kim S. "Quadruped Bounding Control with Variable Duty Cycle via Vertical Impulse Scaling." (IEEE IROS 2014).
[16] Semini, C, et al. "Design of HyQa hydraulically and electrically actuated quadruped robot." J of Sys & Cont Eng (2011).
[17] Ackerman E., (2015 Feb 10). "Spot Is Boston Dynamics' Nimble New Quadruped Robot". Retrieved September 2015 from http://spectrum.ieee.org/automaton/robotics/robotics-hardware/spot-is-boston-dynamics-nimble-new-quadruped-robot.
[18] Farley, C. et al. "Running springs: speed and animal size." Journal of experimental Biology 185.1 (1993): 71-86.
[19] Weyand, Peter G., et al. "Faster top running speeds are achieved with greater ground forces not more rapid leg movements." Journal of applied physiology 89.5 (2000): 1991-1999.
[20] Hudson P et al., "High speed galloping in the cheetah (Acinonyx jubatus) and the racing greyhound (Canis familiaris): spatio-temporal and kinetic characteristics." J exp bio 215.14 (2012): 2425-2434.
[21] Hogan, Neville. "Mechanical impedance of single-and multi-articular systems." Multiple muscle systems. Springer NY, 1990. 149-164.
[22] Blickhan R., and Full R. "Similarity in multilegged locomotion: bouncing like a monopode." J of Comp Phys A 173.5 (1993): 509-517.
[23] Hogan, Neville. "Impedance control: An approach to manipulation." American Control Conference, 1984. IEEE, 1984.
[24] Garcia, Mariano, et al. "Damping and size: Insights and biological inspiration." ISAMAM 2000
[25] Chuah, M, and Kim S. "Enabling force sensing during ground locomotion: A bio-inspired, multi-axis, composite force sensor using discrete pressure mapping." Sensors Journal, IEEE 14.5 (2014): 1693-1703.
[26] Pratt, J et al. "Virtual model control: An intuitive approach for bipedal locomotion." IJRR 20.2 (2001): 129-143.
[27] Bosworth W, Kim S, and Hogan N. "The effect of leg impedance on stability and efficiency in quadrupedal trotting." IEEE IROS 2014